



SEISMIC PERFORMANCE OF RECENTERING BEAM-COLUMN JOINTS REINFORCED WITH SUPERELASTIC SMA BARS AND ECC MATERIALS: EXPERIMENTAL INVESTIGATION AND NUMERICAL SIMULATION

QIAN Hui⁽¹⁾, LI Zongao⁽²⁾, PEI Jinzhao⁽³⁾, KANG Liping⁽⁴⁾, GUO Yuancheng⁽⁵⁾

⁽¹⁾ Professor, School of Civil engineering, Zhengzhou University, Zhengzhou, China, qianhui@zzu.edu.cn

⁽²⁾ Master degree, School of Civil engineering Zhengzhou University, Zhengzhou, China, lizongao@gs.zzu.edu.cn

⁽³⁾ Engineer, Chengdu JiZhunFangZhong Architectural Design Co. LTD., Zhengzhou, China, 1287206015@qq.com

⁽⁴⁾ Doctoral candidate, School of Civil engineering, Zhengzhou University, Zhengzhou, China, 694592871@qq.com

⁽⁵⁾ Professor, School of Civil engineering, Zhengzhou University, Zhengzhou, China, Guoyuancheng@zzu.edu.cn

Abstract

As the key part of the framework structure, the performance of the beam-column joint is crucial to the overall seismic performance of the structure. While it is difficult to achieve the desired results in improving the performance of the frame joints using traditional building materials and solving the residual deformation as well as macro cracks of the structure after strong earthquakes. Shape memory alloys (SMAs) have drawn increasing interest in the field of seismic engineering, due to their unique properties including shape memory effect, superelasticity effect, extraordinary fatigue resistance, high corrosion resistance and high damping characteristics. While, Engineering Cementitious Composites (ECC) is a type of fiber-reinforced concrete, exhibiting high-performance under either tension or shear load. By means of micromechanics design, ECC with a fiber volume fraction of 2% has notable strain-hardening characteristics and the ultimate tensile strain is higher than 3% under the uniaxial tensile load. The combination of SMA and ECC materials enable them widely used in the field of structural seismic engineering.

The objective of this study is to investigate the seismic performance of re-centering beam-column joints with SMA reinforcement and ECC in plastic hinges in improving the capacities of energy-dissipation, deformation and self-repairing, reducing the damage and permanent residual displacement, realizing the rapid recovery of the structural functions after earthquakes. This paper presented a novel recentering beam-column joint reinforced with superelastic NiTi SMA bars and ECC materials. As an alternative of the longitudinal bars in the beam plastic hinge, SMA is used to reduce the residual deformations of the beam while dissipating energy, meanwhile, while the ECC materials used in the critical region of the joint can perfectly solve the brittle nature of concrete and improved the ductility of the structure. Five 1/2 scale frame joints were designed and manufactured according to current Chinese seismic design code, including two SMA-ECC model joints considering the different lengths of SMA bars in plastic hinge region and three contrast joints, namely, normal concrete joint, reinforced ECC joint and SMA reinforced concrete joint. The failure phenomenon, bearing capacity, energy dissipation capacity, displacement, residual deformation as well as the recentering performance of the frame joints were performed under the low reciprocating cyclic loading test. Moreover, the re-centering capacity of the joints with different lengths of SMA reinforcement was also investigated. The finite element model of the joint was built and the numerical simulation analysis of the seismic behavior of the innovative joints under the cyclic loads were carried out. The experimental data and numerical results, including hysteresis curve and skeleton curves, were compared.

Test results show that ECC material are helpful to optimize the development of the plastic hinge at the end of the beam, improving the ductility and energy dissipation capacity of the structure. While SMA bars can dramatically enhance their recentering capability, making the structural damage self-retrofitted, while reducing the initial stiffness and energy dissipation capacity. The SMA-ECC composite system exhibits good interaction, improving significantly the ductility and re-centering capability of the joints and delaying the stiffness degradation speed which can improve the lateral stability of the structure. When the length of the SMA is beyond plastic hinge range, it will not affect the re-centering performance of the joint. The numerical results agree well with experimental data, which shows the reliability and effectiveness of proposed finite element model.

Keywords: Recentering; Beam-Column Joints; Shape Memory Alloy; Engineering Cementitious Composite; Seismic Performance



1. Introduction

The self-centering structure is a new branch of the seismic structural, which will be able to eliminate the permanent deformation of the structure and recover rapidly the structural functions after earthquakes. At present, the self-centering realized primarily by pre-stress technology with steel stranded wire, FRP tendons, carbon fiber tendons and so on. However, these materials, belong to brittleness materials, in the self-centering structure led to a lower ductility and energy absorption. In recent years, it has provided a new idea to solve the above problems with the rapid development of super-elastic shape memory alloy (SMA) and engineering cementitious composites (ECC).

Shape memory alloy (SMA) is a new smart material with the function of self-diagnosis, self-adaptation, self-repair and exhibit unique properties of shape memory effect and superelasticity [1]. The former refers to the deformation suffered below a critical temperature that can be recovered with heating while the latter allows for the recovery of inelastic strains by removal of stress. Superelastic SMA recoverable strain is up to 6%~8%, with a similar yield strength of steel of 400-500MPa, while the ultimate strength and deformation reaching 1000MPa and 25%, respectively. The superelastic characteristic makes SMA have brilliant hysteretic energy dissipation and excellent re-centering capacity [2-8].

Engineering cementitious composites (ECC) is a type of fiber-reinforced concrete and exhibits high-performance under either tension or shear load, which was first introduced by Victor C. Li in University of Michigan in the 1990s [9]. By means of micromechanics design, ECC with a fiber volume fraction of 2% has notable strain-hardening characteristics and the ultimate tensile strain is higher than 3% under the uniaxial tensile load. ECC exhibit distributed cracks with average ultimate tensile crack widths limited to below 100 μm , which make harmful cracks being dispersed into multiple harmless ones. ECC also has better frost resistance and a lower permeability compared to traditional concrete [10-12].

In recent years, SMA-ECC composite material systems than combine excellent ductility, brilliant energy dissipation capacity, extraordinary re-centering capacity, has aroused attention among scholars both at home and abroad. Saiidi *et al.* [13] used SMA longitudinal reinforcement and ECC in the plastic hinge zone of RC bridge columns and evaluated the cyclic response of these columns, the result showed that the average ratio of residual to maximum displacement in the SMA-ECC column was 1/6 of RC column and 1/2 of SMA column, and the highest drift capacity and the least damage were observed in SMA-ECC column. Li *et al.* [14] performed an experimental study on SMA-ECC beam under cyclic flexural loading, showed outstanding energy dissipation capacity, full self-recovery of damage. Through experiments, Hosseini *et al.* [15] demonstrated that using conventional concrete filled prefabricated R/ECC tube with Cu-Al-Mn SEA bars in the plastic hinge region, decreased lateral strength and energy absorption while reduced significantly permanent deformations in columns. Hung *et al.* [16] reported that substituting flexural rebar with Ni-Ti SMA in ECC beam subjected to displacement reversals facilitates the development of plastic hinges and exhibits negligible residual deformation.

This paper presented a novel re-centering beam-column joint reinforced with super-elastic Ni-Ti shape memory alloy and engineering cementitious composites. The prime objective of this study is to investigate the seismic behavior of beam-column joint reinforced with SMA and ECC under cyclic loading, including hysteretic behavior, energy dissipation capacity, ductility, residual deformation re-centering capacity, and so on. And the re-centering capacity of different length SMA reinforcement ECC joints was also observed. The finite element model of the node is established and then do the numerical simulation. The hysteresis curve and skeleton curve are obtained by numerical simulation.

2. Experimental Program

2.1 Test specimens

The objective of the research is to assess the aseismic performance of the exterior beam-column joint element isolated at the points of contraflexure, from a six-story RC building in accordance with current



Chinese seismic design standards. The dimension and arrangement of the specimens were shown in Fig. 1. Five 1/2 scale frame joints elements were designed and manufactured, including three contrast joints (normal

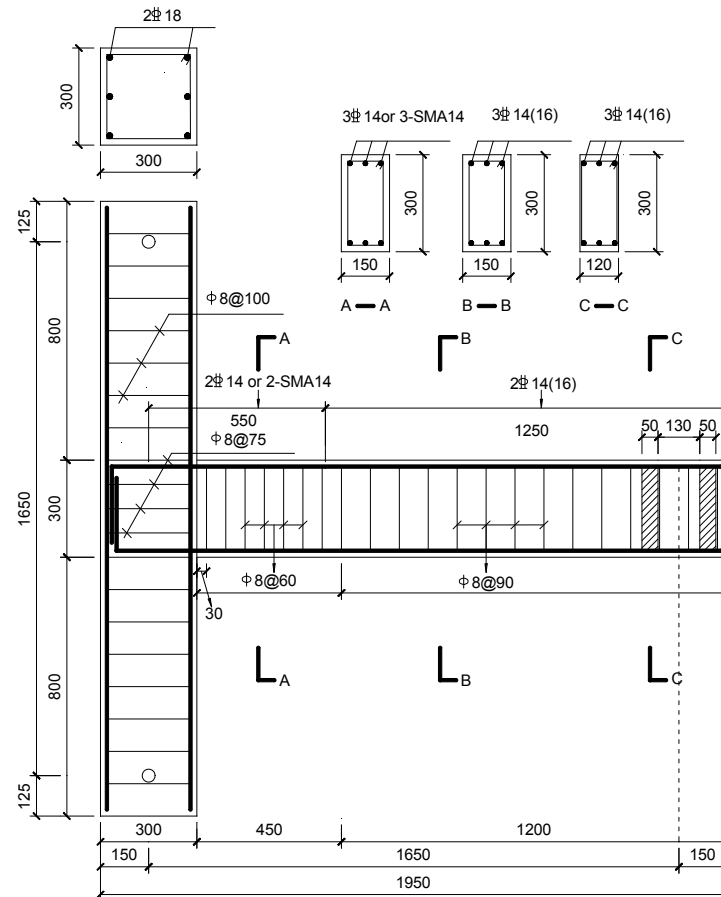


Fig.1 Dimension and arrangement of the specimens

concrete joint, ECC reinforced concrete joint, SMA reinforced concrete joint) and two model joints (different length SMA reinforcement ECC joint). All five specimens had similar geometry and longitudinal and transverse reinforcement arrangements. The cross-sectional dimensions of the columns are 300mm by 300mm reinforced with six bars of 18mm in diameter. As for the beam, whose cross-sectional dimensions are 150mm by 300mm. For the longitudinal reinforcement, six ordinary steel bars of 14mm in diameter are used in JD-R-C and JD-R-ECC. In JD-SMA-C and JD-SMA-ECC-300, six SMA bars of 450mm in length with a diameter of 14mm are used as the substitute of longitudinal reinforcement in the potential plastic hinge zone of the beam. Shorter SMA bars of 375mm in length with the same diameter are used in JD-SMA-ECC-225. In JD-R-ECC, JD-SMA-ECC-225 and JD-SMA-ECC-300, concrete are replaced by ECC in the joint zone and in the potential plastic hinge area of beam and column.

2.2 Material properties

2.2.1 Ni-Ti SMA

Ni-Ti SMA rebar with a diameter of 14mm has been used as reinforcement in this study. To obtain the mechanical properties of these bars (55.86% nickel and 44.14% titanium by weight), dog-bone shaped specimens were tested under cyclic load, as shown in Fig. 2. Fig.3 shows the results of cyclic mechanics performance for the NiTi SMA specimen. The yield point refers to the initiation of phase transformation of SMA is observed as 441 MPa at 0.83% strain. Its elastic modulus was calculated as 66.3GPa, approximately 1/3 of that of reinforced steel. Subjected to a maximum of 6% strain, the SMA specimens exhibited excellent super-elasticity with a residual strain of approximant 0.52%.



2.2.2 ECC Material

The cracking load of ECC material was approximately 4MPa with a cracking strain of 0.02%. The ultimate tensile strain and stress of ECC, with the elastic modulus of 18GPa, were greater than 2.7% and 4.5MPa, respectively. The results showed that the ECC specimens exhibited obvious strain-hardening and multiple cracking properties.



Fig.2 The tensile test of SMA

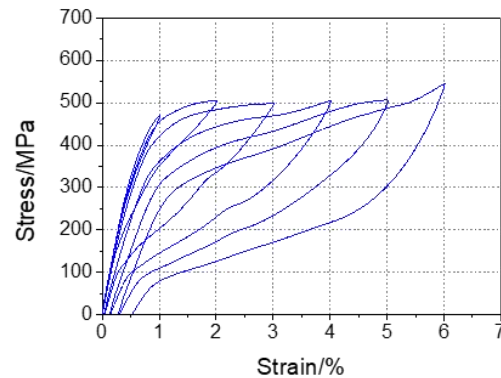


Fig.3 Stress-strain curves of SMA

2.3 Test setup and Loading Protocol

By ignoring the second order effects in the column, the hysteretic properties in the joint core as well as the plastic hinge region of beams were mainly investigated under the reversed quasi-static cyclic load at the beam tip. The top and bottom anti-fleture points of the column are simplified to hinge and roller support separately. The low-cyclic load was applied to the beam tip by an actuator, which hinged reaction wall and between the beam-tip. The photo of the setup during testing was shown in Fig.4.

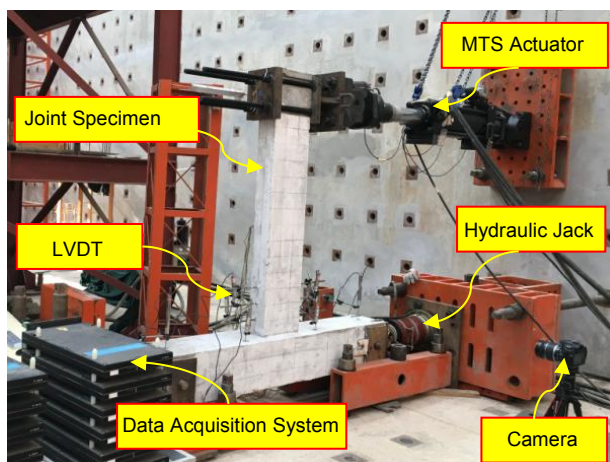


Fig.4 Test setup picture

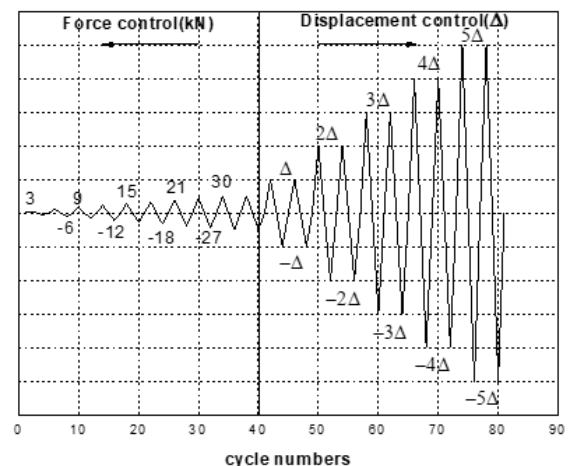


Fig.5 Loading protocol

Fig.5 presents the loading protocol for the experiment. The load history was divided into two stages: load-controlled and displacement-controlled loading phases. Before the theoretical yielding of the specimens, each cycle loaded the beam tip with an incrementally increasing load value of 3 kN. After that, horizontal reversed cyclic displacements, incremented by the yield displacement (Δ), were repeated twice at each drift level until the failure of the specimen.



3. Experimental Results

The seismic performance of beam-column joints reinforced with SMA and ECC is evaluated via damage patterns, load-deformation relationship, maximum crack width at peak displacement and after unloading, residual deformation, energy dissipation capacity, curvature-rotation relationship, stiffness degradation.

3.1 Damage patterns

Close-up images of the plastic hinge area of each joint at the final damage are presented in Fig.6. In all specimens, without diagonal cracks in joint core were observed, most of the flexural cracks were developed in the beam member from the column face to beam tip and concentrated upon the beam near the column face. It can be seen in Fig.6(a), (b) that in JD-R-C and JD-R-ECC plastic hinges, where ECC or concrete was seriously crushed, were formed in the beam for a distance of 300 mm from the edge of the column. While, protective layers spall and steel reinforcement exposure were observed in JD-R-C, not in JD-R-ECC. See Fig.6(c), (d) and (e). Shorter plastic hinges on beam end appear in JD-SMA-C and JD-SMA-ECC. As for JD-SMA-C, the significant concrete spalled in both the cover and core regions was concentrated on the beam end within a length of 50 mm near the column face, and the width of all other cracks in the beam are very small. Whereas, the horizontal penetrating cracks almost parallel to the column face were just created in the beam end in both two JD-SMA-ECC, which were noticed plentiful hairline cracks vicinity of main crack and ECC is not crushed.

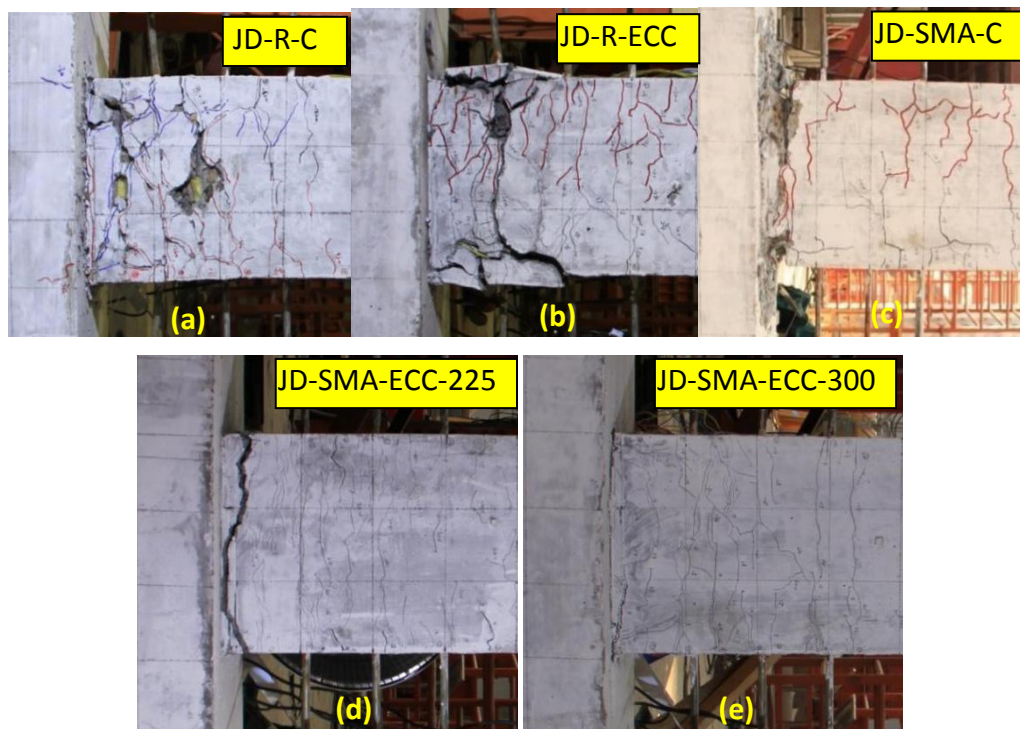


Fig.6 Damage patterns of the specimens

3.2 Load-displacement hysteretic results in beam-joint test

Fig.7 presents the load-displacement hysteretic loops of all specimens. See Fig.7(a) and (b), JD-R-C and JD-R-ECC exhibit very similar hysteretic properties, whose hysteretic curves are in plump shapes and have no significant pinch phenomenon. However, the ultimate lateral force developed in JD-R-ECC was slightly higher compared to JD-R-C. Large permanent displacement at beam tip was observed in both two joints after it is fully unloaded in each loading cycle. As shown in Fig.7(c), (d) and (e), when the reinforcement steel in the potential plastic hinge area of the beam is replaced by SMA bar, the desired behavior with flag-shaped hysteretic curve is possessed by JD-SMA-C and JD-SME-ECC. Obviously, this has resulted in extremely

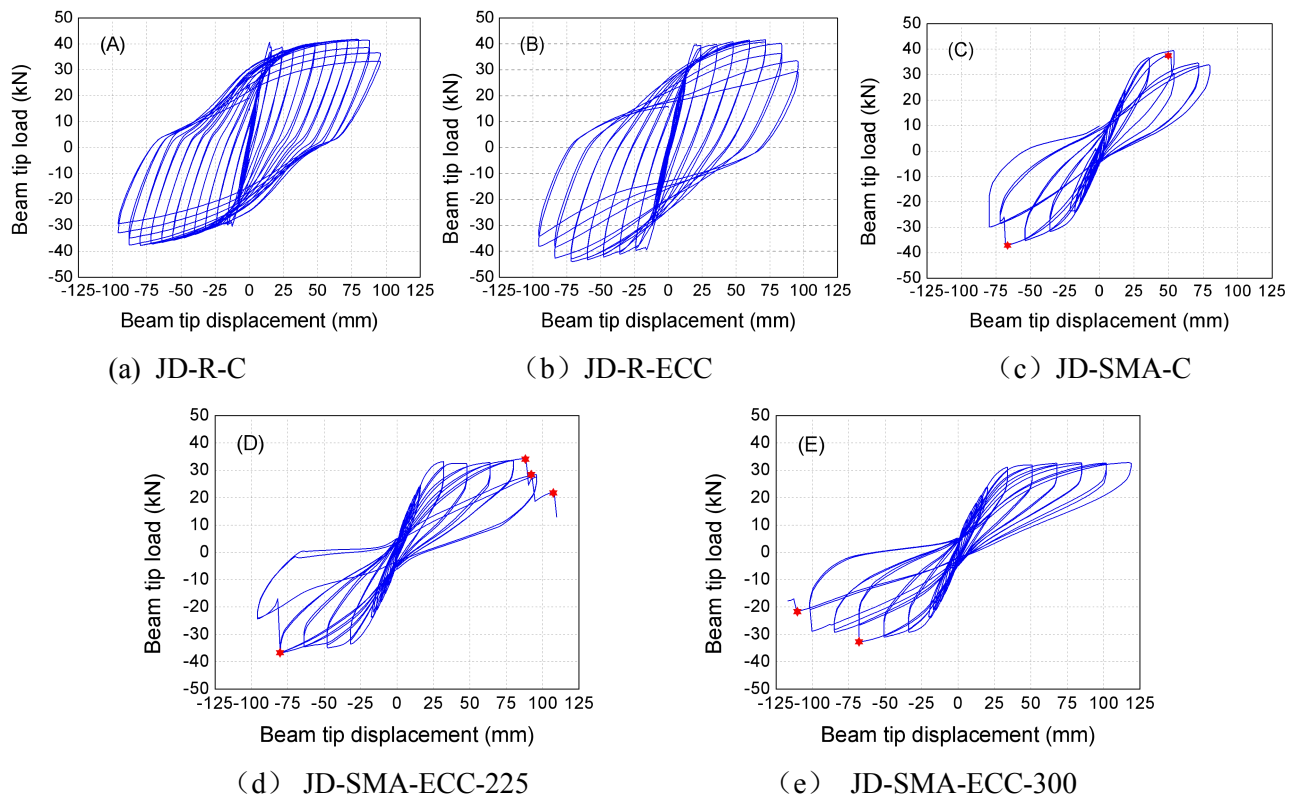


Fig.7 Hysteresis loops and spine curves of the specimens

small permanent deformation and a reduced area within the hysteresis loops, implying that SMA material can improve significantly the re-centering capability but reduce the energy dissipation capacity of joints. Larger deformation went through by JD-SMA-ECC compared to JD-SMA-C before the failure, suggesting that the significantly improved structural ductility of ECC over the normal concrete. Up to the rupture of screw of SMA bar, similar maximum bearing capacity and re-centering capability of JD-SMAECC-225 and JD-SMAECC-300 indicates that shortening the length of SMA bars in the potential plastic hinge area of beam does not decrease hysteretic behavior of joints. This contributes to reduce the dosage and costs of SMA material.

3.3 Skeleton curves

Skeleton curve reflects mechanics performance of specimens in elasticity phase, plasticity phase and the damage phase, and provides an important basis for elastoplastic seismic response analysis of structure. The skeleton curve of each joint is given in Fig. 8. It can be seen that during the initial loading period, the skeleton curve of both JD-R-ECC and JD-R-C are basically in coincidence, while with the increasing of lateral load, smaller slope of skeleton curve appeared in JD-R-ECC. The yielding strength and ultimate strength improved in JD-R-ECC compare to JD-R-C, indicating that the structures, where the normal concrete in the critical area is replaced by ECC, possess improved ductility and delayed yielding. It is also noted that the slope of skeleton curve of joints reinforcement with SMA bars is obviously less than normal concrete joint's and ECC reinforced concrete joint's, suggesting SMA bar will lead to a decline in the initial stiffness of the structure. This is because the elastic modulus of SMA (70.5GPa) is much less than that of reinforcement steel (approximately 205GPa). The yield displacement at beam tip was reduced compare to the normal concrete joint for all specimens ranging from approximately 28%–45%, as a result of lower stiffness of ECC and SMA. Remarkably, although the ultimate bearing capacity of JD-SMA-ECC degrades by approximately 10% compared to JD-SMA-C, the strength retention capability of JD-SMA-C remains fantastic.

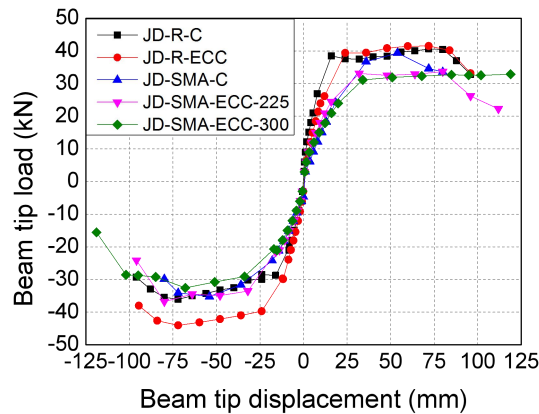


Fig.8 Skeleton curves of the specimens

3.4 Residual deformation of beam tip

The permanent displacement at beam tip as a function of maximum experienced displacement is also provided in Fig.9. As seen from this figure, the permanent displacement at the beam tip for all specimens exhibited an approximately linear increase with increasing maximum experienced displacement. However, all the joints reinforced with SMA bars have a negligible permanent displacement at beam tip after it is fully unloaded in each loading cycle. In particular, with a beam tip experienced deformation of 80mm, the recoverable deformation of JD-SMA-ECC was up to 83%, while this value was reduced to approximately 35% for the JD-R-C and JD-R-ECC. Although one of the connectors between steel bar and SMA bar ruptured prematurely (with a peak beam tip deformation of 54 mm), the recoverable deformation of JD-SMA-C still reaches to 73%, slightly less than JD-SMA-ECC. The results imply that ECC structure longitudinally reinforced with Ni-Ti SMA bars can be expected to achieve the desirable characteristics for structural ‘resilience’.

3.5 Energy dissipation capacity

The energy dissipation as a function of maximum experienced displacement is given in Fig.10. Despite lower compressive strength of ECC (35.3MPa) compare to concrete (44.8MPa) in this study, the energy absorption was very similar in JD-R-C and JD-SMA-ECC. This indirectly indicates that ECC members possess more excellent energy absorption capacity than concrete members with equal strength. Due to the outstanding super-elastic nature of SMA material, a lower energy dissipation capacity was observed in joints longitudinally reinforced with SMA bars. When the experienced displacement of the beam tip up to 75mm, the energy absorption in JD-SMA-ECC is about 40% of that of JD-R-C and JD-R-ECC, and slightly lower than that of JD-SMA-C.

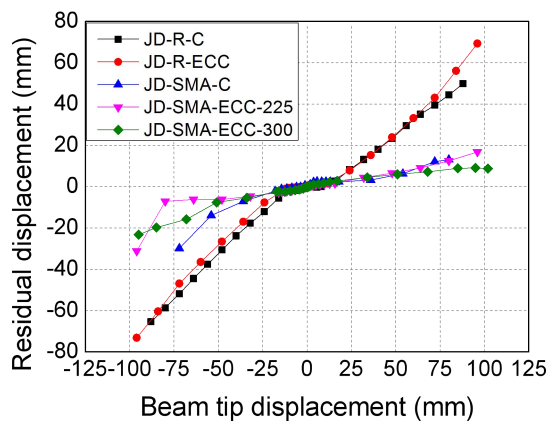


Fig.9 Residual displacement of the beam tip

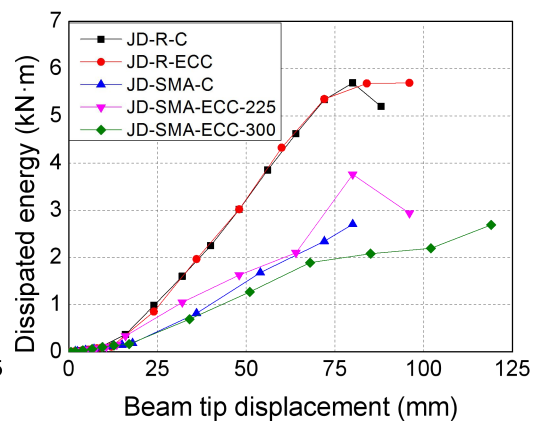


Fig. 10 Energy dissipation capacity



4. Numerical Simulation

4.1 Finite element model

4.1.1 Material model

SMA material selection OpenSEES Self-centering constitutive model [15]. This constitutive model is defined with seven parameters as shown in Tab.1, and it has the characteristic of flag hysteric, as shown in Fig.11. The ECC material was selected from the constitutive model of ECC01 developed by Tong-Seok Han [16]. It is a corotational total strain-based constitutive model for ECC, as shown in Fig.12, and the parameters used are shown in Tab.2 The constitutive model is capable of describing the complex cyclic behavior of ECC with reasonable accuracy.

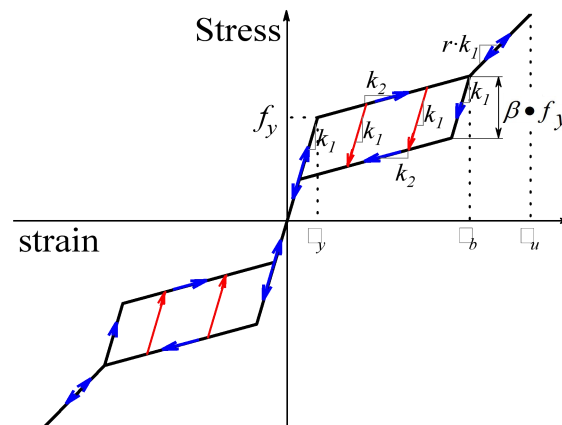


Fig.11 Constitutive model of SMA

Tab. 1 The parameters and values of SMA

| Parameters | Values | Unit |
|-----------------|--------|------|
| k_1 | 40000 | Mpa |
| k_2 | 1827 | Mpa |
| f_y | 400 | Mpa |
| β | 0.8 | - |
| ε_s | 0.06 | - |
| ε_b | 0.06 | - |
| r | 1 | - |

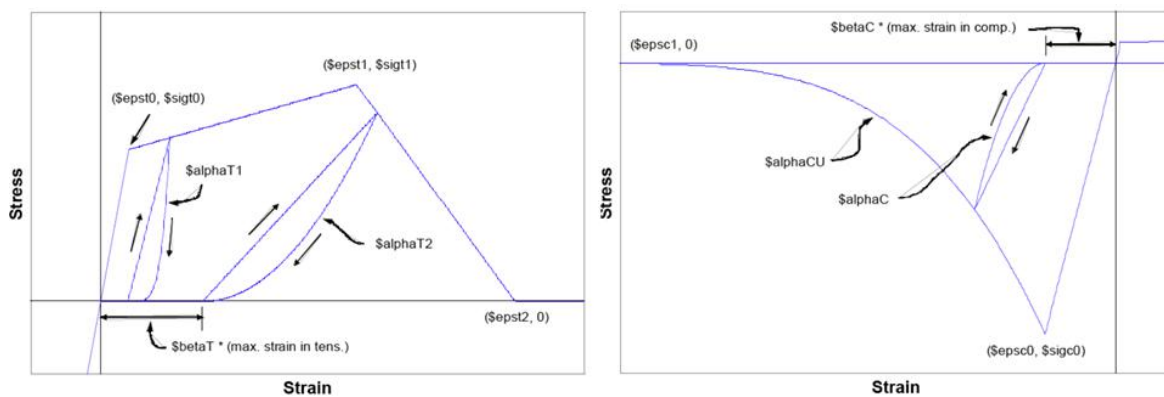


Fig.12 Constitutive model of ECC



Tab. 2 The parameters and values of ECC01

| Parameters | Values | Parameters | Values |
|------------|----------|------------|--------|
| $t0$ | 3.8Mpa | $sc1$ | -0.012 |
| $st0$ | 0.00025 | $T1$ | 2 |
| $t1$ | 4 Mpa | $T2$ | 2 |
| $st1$ | 0.037 | C | 5 |
| $st2$ | 0.06 | CU | 1 |
| $c0$ | -26.8Mpa | T | 0.4 |
| $sc0$ | -0.005 | C | 0.3 |

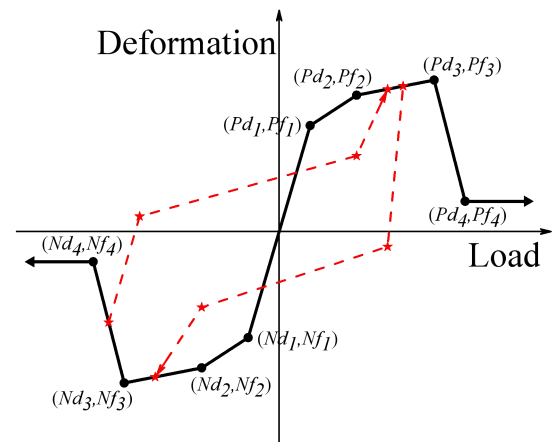
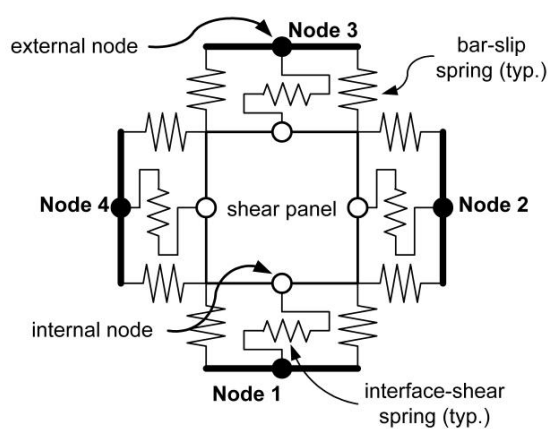


Fig.13 Macroscopic mechanical model of joints Fig.14 Hysteretic one-dimensional load-deformation model

Reinforcement model based on Chang and Mander uniaxial steel model (Reinforcing-Steel). This model can better simulate the stiffness degradation of reinforcement due to fatigue and yield. The concrete model adopts the Kent-Park concrete constitutive model "concrete01" model. Based on the Kent-Park model, this model considers the constraint effect of stirrup.

4.2.2 Beam-column joint model

The "beam-Column-Joint" model, proposed by Lowes and improved by Mitra [17], can better show the stress characteristics of beam and column joints. The joints model adopts three components to simulate the three main failure modes at the joints. Shear panel is used to simulate shear failure in core area. The zero-length bar-slip spring is used to simulate bar-slip failure between reinforcement and concrete. The zero-length interface-shear spring simulates shear failure around the node, as shown in Fig.13.

The shear plate element is "Pinching4". The one-dimensional load-deformation hysteretic model is based on MCFT theory. The shear stress-strain relationship in the core zone of the joints is calculated with this theory, as shown in Fig.14. The bar-slip model of reinforcement is bar-slip material based on this model. According to the parameters of reinforced concrete in the joint area, the slip spring model is obtained. The interface-shear spring is defined as an elastic spring with infinity elastic modulus. This is because the shear stiffness at the interface of the Cast-in-situ joints is relatively large, which is all within the elastic range.

4.2 Numerical Results

The parameters of each material and element in the finite element model are determined according to the parameters obtained from the material experiment. According to the actual displacement of each component in each cycle during the experiment, displacement control is adopted for loading. Compare simulation data with experimental data on hysteresis curve. Verify the correctness and applicability of finite element model.

The numerical simulation results are shown in Fig.15. In Fig15(a), the experimental and simulated

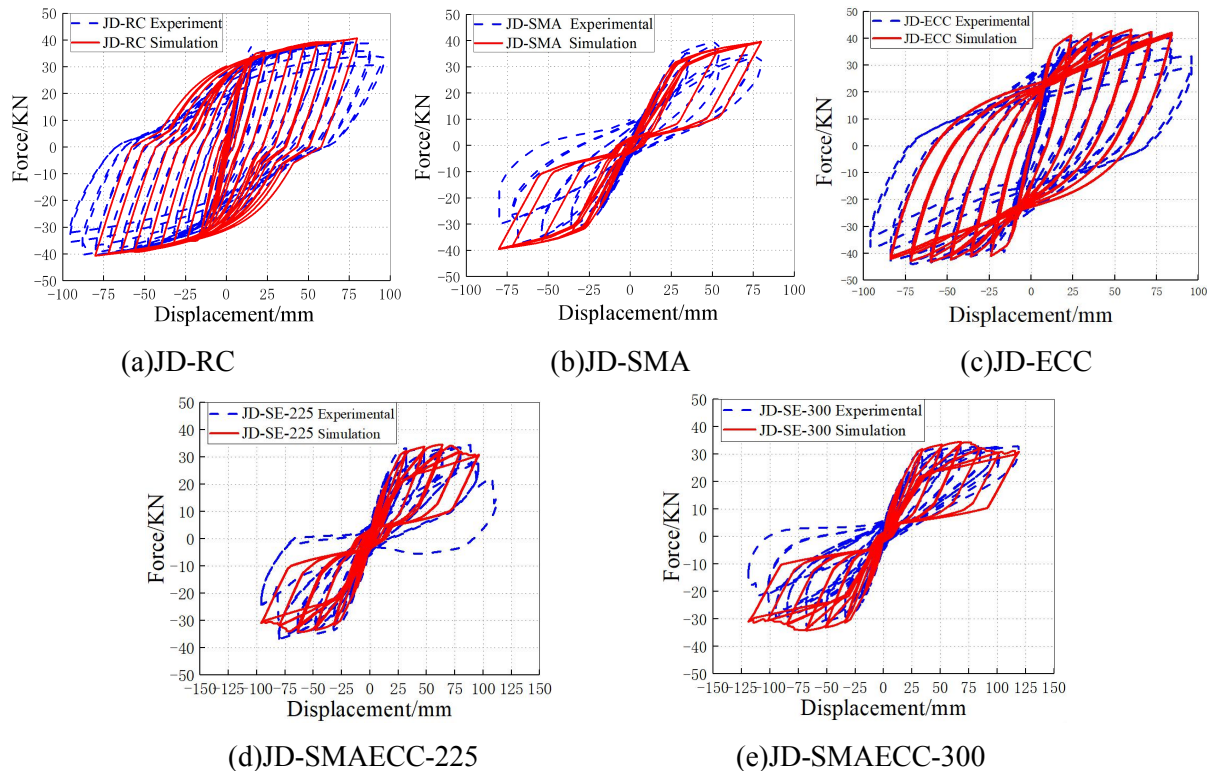


Fig.15 Comparisons between the simulation results and experimental data

curves are consistent. This shows that the “beam-Column-Joint” model is effective. In Fig15(b) and 15(c), SMA model and ECC model can simulate the hysteretic performance of joints well. Based on the correctness of these models, in Fig15(d) and 15(e), SMAECC joints simulation also achieves consistent results.

5. Conclusions

This paper presented an experimental investigation and numerical study of the seismic performance of a novel re-centering beam-column joint reinforced with super-elastic Ni-Ti SMA and ECC. Test results show that ECC material are helpful to optimize the development of the plastic hinge at the end of the beam, improving the ductility and energy dissipation capacity of the structure. While SMA bars can dramatically enhance their recentering capability, making the structural damage self-retrofitted, while reducing the initial stiffness and energy dissipation capacity. The SMA-ECC composite system exhibits good interaction, improving significantly the ductility and re-centering capability of the joints and delaying the stiffness degradation speed which can improve the lateral stability of the structure. When the length of the SMA is beyond plastic hinge range, it will not affect the re-centering performance of the joint. The numerical results agree well with experimental data, which shows the reliability and effectiveness of proposed finite element model.

6. Acknowledgements

The research reported in this paper was supported by National Science Fund of China (NSFC) through Grant No.51478438 and No.51978631. The supports are greatly appreciated.

References

- [1] Song G, Mo Y L, Otero K and Gu H. Health monitoring and rehabilitation of a concrete structure using intelligent materials[J]. Smart Material and Structure. 2006, 15: 309 – 314



- [2] Youssef M A, Alam M. S, Nehdi M. Experimental investigation on the seismic behavior of beam-column joints reinforced with superelastic shape memory alloys[J]. *Journal of Earthquake Engineering*, 2008, 12: 1205~1222
- [3] Zhang, Y. and Zhu, S. A shape memory alloy-based reusable hysteretic damper for seismic hazard mitigation[J]. *Smart Mater. Struct.*, 2007 .16:1603 - 1613.
- [4] DesRoches R, Delemont M. Seismic retrofit of simply supported bridges using shape memory alloys[J]. *Engineering Structures*, 2002. 24: 325-332.
- [5] Qian Hui, Li Hongnan, Song Gangbing. Experimental Investigations of Building Structure with a Superelastic Shape Memory Alloy Friction Damper Subject to Seismic Loads[J]. *Smart Material and Structure*, 2016, 25:125026, 1-14.
- [6] Qian Hui, Li Hongnan, Song Gangbing ,et al. Recentering Shape Memory Alloy Passive Damper for Structural Vibration Control[J]. *Mathematical Problems in Engineering*. vol. 2013, Article ID 963530, 1-13, 2013.
- [7] Saiidi M S, O'Brien M and Sadrossadat-Zadeh M. Cyclic response of concrete bridge columns using superelastic Nitinol and bendable concrete[J]. *ACI Structural*.2009,106 69-77
- [8] Tazarv M, Saiidi MS. Reinforcing NiTi Superelastic SMA for Concrete Structures[J].*Journal of Structural Engineering*.2015;141(8):1-10.
- [9] Li V C. Performance driven design of fiber reinforced cementitious composites [C]// Swamy R N. *Proceedings of 4th RILEM International Symposium on Fiber Reinforced Concrete*. Chapman and Hall, 1992: 12-30.
- [10] Boshoff W P. Cracking behavior of strain-hardening cement based composites subjected to sustained tensile loading *ACI Mater. J.* 2014, 111(5), 53-60
- [11] Shin S K, Kim J J H, Lim Y M. Investigation of the strengthening effect of DFRCC applied to plain concrete beams[J]. *Cement and Concrete Composites*, 2007, 29(6): 465-473.
- [12] Li Xiaopeng, Li Mo and Gangbing Song. Energy-dissipating and self-repairing SMA ECC composite material system[J]. *Smart Materials and Structures*, 2015, 24(2) :1-15
- [13] Hosseini F, Gencturk B, Lahpour S et al. An experimental investigation of innovative bridge columns with engineered cementitious composites and Cu-Al-Mn super-elastic alloys[J]. *Smart Materials and Structures*, 2015,24:085029
- [14] Hung Chung-Chan, Yen Wei-Ming, Yu Kun-Hao. Vulnerability and improvement of reinforced ECC flexural members under displacement reversals: Experimental investigation and computational analysis[J].*Construction and Building Materials*, 2016,107 :287-298
- [15] Kunnath SK, Heo Y, Mohle JF. Nonlinear Uniaxial Material Model for Reinforcing Steel Bars[J]. *Journal of Structural Engineering*. 2009;135(4):335-343.
- [16] Han TS, Feenstra PH, Billington SL, Simulation of Highly Ductile Fiber-Reinforced Cement-Based Composite Components Under Cyclic Loading, *ACI Structural Journal*, V100, No. 6, pp. 749-757.
- [17] Lowes L N, Mitra N, Altoontash A M.A beam-column joint model for simulating the earthquake response of reinforced concrete frames. *Pacific Earthquake Engineering Research Center, College of Engineering, University of California*, 2003.